Eur. Phys. J. AP **5**, 231–236 (1999)

THE EUROPEAN PHYSICAL JOURNAL APPLIED PHYSICS

On the relation between Frank-Read source nature and fine slip line structure

C. Coupeau and J. Grilhé[a]

Laboratoire de Métallurgie-Physique[b], Université de Poitiers, UFR Sciences, Bâtiment SP2MI, B.P. 179, 86960 Futuroscope Cedex, France

Received: 15 December 1997 / Revised: 18 September 1998 / Accepted: 15 December 1998

Abstract. Slip patterning is influenced by both the distribution of Frank-Read sources in the bulk crystal and the dislocation interactions before emerging at the surface. The fine structure of slip lines is also highly dependent on the intrinsic nature of Frank-Read sources and particularly on their pinning points and external dislocation network, which is often not considered. In this paper, different types of Frank-Read sources are reviewed and the direct effects are described and discussed of these dislocation multiplication mechanisms on the step fine structure at the surface.

PACS. 61.72.Bb Theories and models of crystal defects – 61.72.Hh Indirect evidence of dislocations and other defects (resistivity, slip, creep, strains, internal friction, EPR, NMR, etc.)

1 Introduction

Over the past decade, scanning probe microscopes (SPM) have attracted considerable attention since they enable real-space examination of atomic scale details on surfaces [1–5]. The atomic force microscopy (AFM) does not depend on sample conductivity for image acquisition, and so applies equally well to insulating or conductive samples; this is not the case with scanning tunneling microscopy (STM). AFM has been proven recently to be particularly suited to the analysis of the fine slip line structure on a nanometer scale [6–9] with occasionally a fractal tendency of slip line patterning [10]. Moreover the coupling of a micro-compression machine to an AFM enables the in situ study of the dislocation emergence process at the surface from the early stage of plastic deformation to work-hardening [11,12]. The emergence of the first few dislocations, formation, growth and widening of slip line patterning can be investigated [13]. A temperature controlled microstage [14,15] has also been developed recently and provides a new dimension to the application of AFM to the study of phase transitions, thermal-activated surface phenomena, and more generally plastic deformation mechanisms. The atomic resolution offered by this class of microscopy enables an accurate study of Frank-Read source activation and subsequent effects generated at the surface on a nanometer scale.

In general, slip patterning is characterized by the degree of slip localization and it is now well-known that slip line structure depends on the distribution of sources with-in the bulk crystal, as well as interactions of dislocations gliding through the bulk before emerging at the surface. Temperature, stacking fault energy and nature of obstacles to dislocation motion are parameters playing an important role in the organization of slip patterning [16]. Simulations have been realized, taking into account some specific parameters such as source distribution and efficiency, and plastic deformation processes with mainly cross-slip and annihilation [17,18].

Since Frank and Read [19], it is also well-known that the fine slip line structures is strongly dependent on the intrinsic nature of the so-called Frank-Read sources, and particularly on their anchorage points, that is, the external dislocation network. As an example of the fine structure of slip pattern, an AFM image is presented in Figure 1. These image has been taken in ambient air and the enclosed cross section perpendicular to the slip line structure shows the potential of this technique to give interesting information about the nature of the Frank-Read sources. In this paper, these different types of sources are reviewed and direct effects of these various sources on the step fine structure at the surface are described subsequently.

2 Nature of Frank-Read sources

The following configuration has been studied with a dislocation segment A-B which is a potential source of dislocations. This dislocation has a $\mathbf{b}_3$ Burgers vector so that plane $P(\mathbf{b}_3,\ \mathbf{l}_3)$ [20,21] is the only possible glide plane

[a] e-mail: grilhé@lmp.univ-poitiers.fr
[b] UMR 6630 CNRS

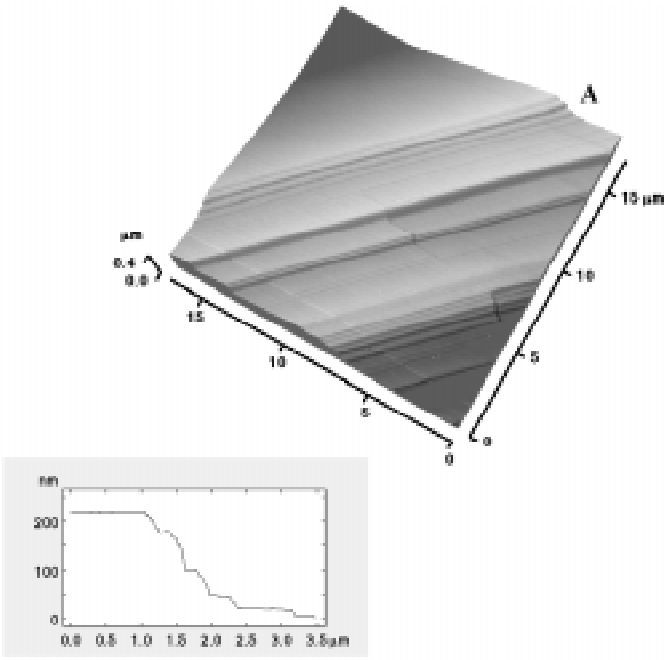

Fig. 1. Topographical AFM image of the fine slip line structure of a Ni based superalloy phase γ single crystal. The sample has been deformed up to 1.03%. A profile plot of the step structure labeled A, obtained by averaging few consecutive sections perpendicularly to the slip lines, is presented.

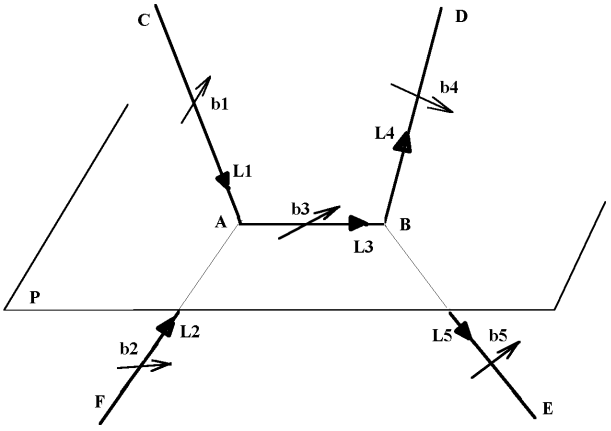

Fig. 2. Schematic diagram of external dislocation network around a potential dislocation source A-B. The associated slip plane is labeled P. Each dislocation (i) is symbolized by its line direction $\mathbf{L}_i$ and Burgers vector $\mathbf{b}_i$.

and is encompassed with four other dislocations CA, FA, DB and EB with $\mathbf{b}_1$, $\mathbf{b}_2$, $\mathbf{b}_4$ and $\mathbf{b}_5$ Burgers vectors respectively (Fig. 2). (CA) can only move in plane $\mathrm{Q}(\mathbf{b}_1, \mathbf{l}_1)$ which induces a displacement of A only along line D corresponding to the intersection of P and Q. Likewise, because of dislocation (FA), A is restricted to line $D' = P \cap R$. A is therefore a fixed point and acts as anchorage for dislocation (AB) (Fig. 3). A similar behaviour is expected for point B. At these two points, the following equations

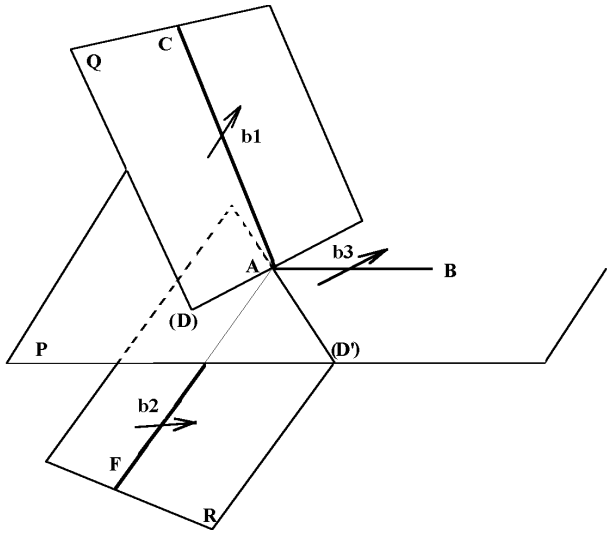

Fig. 3. Dislocations CA and FA are restricted to move in planes Q and R respectively. Point A is the intersection of lines D and D' and acts therefore as pinning point for the dislocation source. A similar behaviour occurs at point B.

apply:

$$\mathbf{b}_3 = \mathbf{b}_1 + \mathbf{b}_2,$$
$$\mathbf{b}_3 = \mathbf{b}_4 + \mathbf{b}_5.$$

By projecting each Burgers vector along directions perpendicular and parallel to slip plane P, one obtains (Eq. (1)):

$$\begin{aligned} b_{3\perp} &= 0 = b_{1\perp} + b_{2\perp}, \\ b_{3\perp} &= 0 = b_{4\perp} + b_{5\perp}, \\ b_{3\parallel} &= b_{1\parallel} + b_{2\parallel}, \\ b_{3\parallel} &= b_{4\parallel} + b_{5\parallel}. \end{aligned} \tag{1}$$

Moreover, the formation of such a dislocation network from the interaction of two dislocations with the subsequent creation of junctions in-between, induces the following conditions (Eq. (2)):

$$\begin{aligned} \mathbf{b}_1 &= \mathbf{b}_5 \quad (\text{or } \mathbf{b}_4), \\ \mathbf{b}_2 &= \mathbf{b}_4 \quad (\text{or } \mathbf{b}_5). \end{aligned} \tag{2}$$

It is worth noting that all Burgers vector perpendicular components are equal:

$$\forall i, \ |b_{i\perp}| = K.$$

With equations (1), one obtains:

$$b_{1\perp} = b_{4\perp} = -b_{2\perp} = -b_{5\perp} \equiv b_\perp.$$

In the case of $K = 0$, the slipping of dislocation (AB) is confined to P and remains purely planar. This mechanism corresponds to the first model of Frank-Read [19,22–24] with successive expansion under stress of the initial dislocation, symmetrical rolling up around dislocation nodes

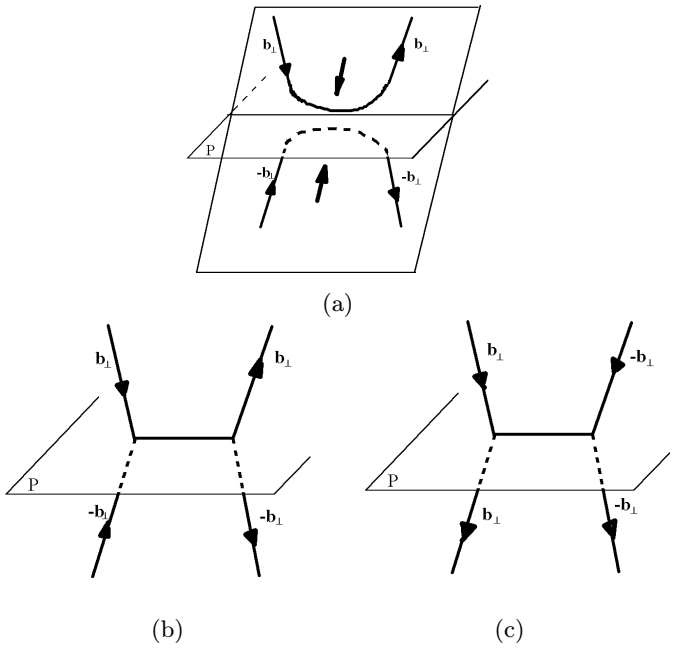

Fig. 4. Configuration $\mathbf{b}_1 = \mathbf{b}_4$ and $\mathbf{b}_2 = \mathbf{b}_5$, resulting from the recombination of dislocations at the intersection of their slip planes. Each dislocation is here represented by its Burgers vector component perpendicular to plane P and an arrow indicates the direction of the slip line: (a) origin of studied dislocation network; (b) schematic configuration; (c) equivalent configuration by FSRH consideration.

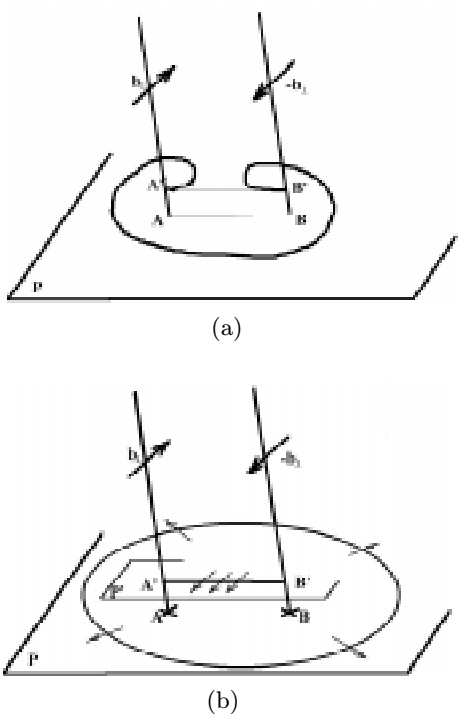

Fig. 5. Activation process of *movable Frank-Read source*. (a) In a first step, the initial dislocation AB expands on crystallographic plane P under the applied stress and rolls up around its pinning points. A climb up of dislocation is observed by a same amount at A and B resulting from the nature of the external dislocation network. (b) After an almost entire revolution around A and B, dislocation recombination occurs. The initial dislocation segment has climbed up in a parallel crystallographic plane whereas a dislocation loop expands in the first slip plane. This process is hence regenerative with a new potential source at $b_\perp$ distance from the first one.

A and B, and finally recombination with a new potential dislocation source. This mechanism may thus be labeled as a *planar Frank-Read source*. From this model, extensions have been developed, for instance, models to explain twinning [25–27].

It is now well-known that a screw (or mixed) dislocation transforms the lattice plane into an helical plane turning around the dislocation with a path equal to its screw Burgers vector component $b_\mathrm{v} = b_\perp$. This helice is right or left depending of the sign of the Burgers vector. So, in the case of $K \neq 0$, by expanding in these gliding surface, the dislocation climbs with a step equal to $b_\perp$ after each revolution around the pinning point A. Moreover as $\mathbf{b}$ is a Bravais lattice vector, $b_\perp$ corresponds to a distance between to two parallel planes (parallel to P).

In the case of $K \neq 0$, two different cases are now examined. The first case ($\mathbf{b}_1 = \mathbf{b}_4$ and $\mathbf{b}_2 = \mathbf{b}_5$) corresponds to the recombination of two dislocations at the intersection of their respective gliding planes (Fig. 4a). With equations (1), one obtains:

$$b_{1\perp} = b_{4\perp} = -b_{2\perp} = -b_{5\perp} \equiv b_\perp.$$

Each dislocation is represented by its Burgers vector component perpendicular to the plane P and its line defined by an arrow (Fig. 4b). By FS/RH convention, two dislocations are similar if they have a similar $\mathbf{b}$ and $\mathbf{l}$. The equivalent configuration is therefore seen in Figure 4c. As for the Frank-Read model, the dislocation is held at both ends and tends to bow out under an applied stress. The dislocation then continues to expand but climbs locally around anchorage points A and B (Fig. 5a). In this case, the Burgers vector opposite signs and the opposite rotary motion around each dislocation of external network explain that the climb-step is the same at A and B, equal to $b_\perp$ as described previously. This mechanism occurs in the same direction only in the upper area of slip plane P. After a complete spiraling around A and B, dislocation segments then meet and annihilate one an other because of their positive and negative orientations, as in the case of planar sources. A wide loop is formed and can extend all over the crystal. A Burgers circuit distant from these dislocations verifies that the crystal remains perfect in regards to the surface perpendicular direction and that the dislocation loop from the initial segment A-B can glide in planar P. The process is obviously regenerative, as for a planar Frank-Read source, except that the new dislocation is created in plane P' parallel to P at a distance $b_\perp$ (Fig. 5b). Hence, instead of a planar mechanism, a series of loops is produced with only one dislocation every crystallographic plane. The corresponding source is the so-called *movable Frank-Read source*.

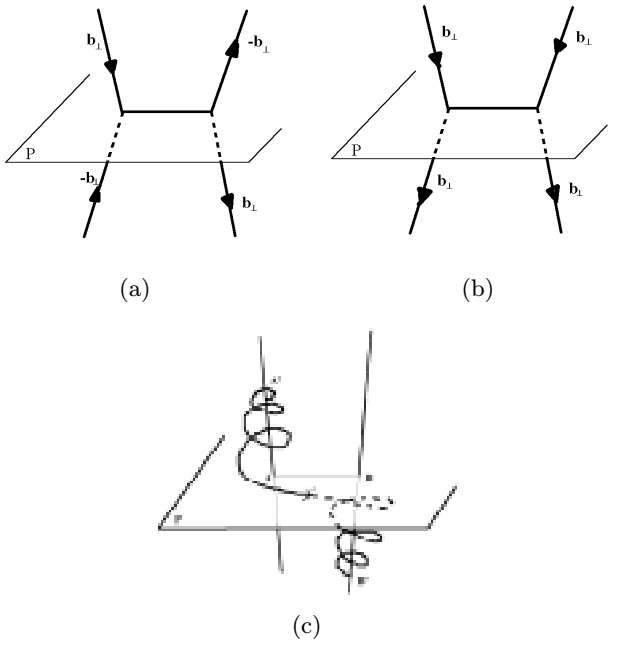

Fig. 6. Activation of *helical Frank-Read source*. (a) Configuration of external dislocation network issued from dislocation interaction with the further creation of junction in-between. (b) Equivalent configuration by FRSH convention. (c) Behaviour of the initial dislocation segment A-B under stress. *As movable Frank-Read source*, the dislocation expands and wraps up around A and B points, but on both sides of slip plane P, which prevents subsequent recombination.

The second configuration ($\mathbf{b}_1 = \mathbf{b}_5$ and $\mathbf{b}_2 = \mathbf{b}_4$) results from dislocation interaction with the creation of a dislocation in-between. The following relation is also obtained:

$$b_{1\perp} = b_{5\perp} = -b_{2\perp} = -b_{4\perp} \equiv b_\perp.$$

As previously defined and described, the configuration of the dislocation network and the equivalent one by FS/RH are represented in Figures 6a and 6b respectively. Contrary to the previous mechanism, dislocations in the upper area of slip plane P are here identical, which induces a highly different behaviour for segment A-B under an applied stress. Indeed, in this case, the spiraling of the initial dislocations around A and B occurs on both sides of plane P so that no subsequent recombination is possible. The multiplication of dislocations is here ensured by a pole mechanism and creation of a double helix. This kind of dislocations has obviously been observed in crystals which have been previously thermally treated to produce climb conditions, which is not the case in our study. Each revolution around A and B nodes produces a further spiral in the helix, acting each time as a new dislocation (Fig. 6c). The associated mechanism is also called the *helical Frank-Read source*.

In the following paragraph, the effects generated at the surface are described for each specific Frank-Read source activation. The influence of forest interaction on slip line structure is also briefly discussed, with the creation of *multiple spiral sources* which certainly represents the main contribution at relatively long range of *slip line swarming*, that is, high multiplication of slip lines at surfaces.

3 Slip line fine structure

3.1 Role of the nature of Frank-Read sources

The emergence at the surface of one dislocation creates a step whose unit height depends only on its Burgers vector and is equal to its projection perpendicular to the surface:

$$h_e \equiv b_\perp = \mathbf{b} \cdot \mathbf{n}.$$

In the first model of Frank-Read source, the mechanism of dislocation multiplication is purely planar and a series of loops is produced in the same crystallographic plane. Thus, a step is created at the surface of height increasing uniformly whilst the emergence process is activated. The *in situ* examination of step fine structure and evolution under stress may give interesting information about the activation life of Frank-Read sources before further locking.

In the case of movable Frank-Read sources, it is shown that only one dislocation is produced. This mechanism occurs after each revolution around A and B nodes in a neighbouring parallel plane. Assuming that there is no interactions in the bulk, the motion of dislocations and subsequent emergence at the surface induces the creation of a monoatomic step series of uniform height. It must be emphasized that the widening of the associated slip line structure is asymetric, with a fixed side linked to the initial position of the Frank-Read source in the bulk crystal (Fig. 7a).

In regards to helical Frank-Read source, a similar behaviour is expected with the development of a slip band at the surface, composed of monoatomic steps, but on both sides of the first generated step (Fig. 7b).

3.2 Role of the forest crossing

Dislocations moving in a given slip plane may intersect dislocations crossing this slip plane. This well-known mechanism called interaction with forest dislocations [28–30] results in the creation of many jogs along the dislocation lines. Many cases have been studied in the past, depending primarily on the Burgers vector of the intersecting dislocations. The influence of lattice friction, temperature, strain-rate, cross-slip ability and precipitation has also been discussed [31]. A dislocation AB with Burgers vector $\mathbf{b}$ and containing a jog CD will expand under an applied stress in its primary slip plane. The jog CD is a sessile dislocation and acts as pinning points for the mechanism. Involving a pole mechanism, dislocations AC and BD wrap up in their respective slip planes P and P', giving rise to a double spiral sources (Fig. 8). It is therefore clear that any jog along dislocation lines is a potential source of dislocations, so-called *multiple spiral Frank-Read source*.

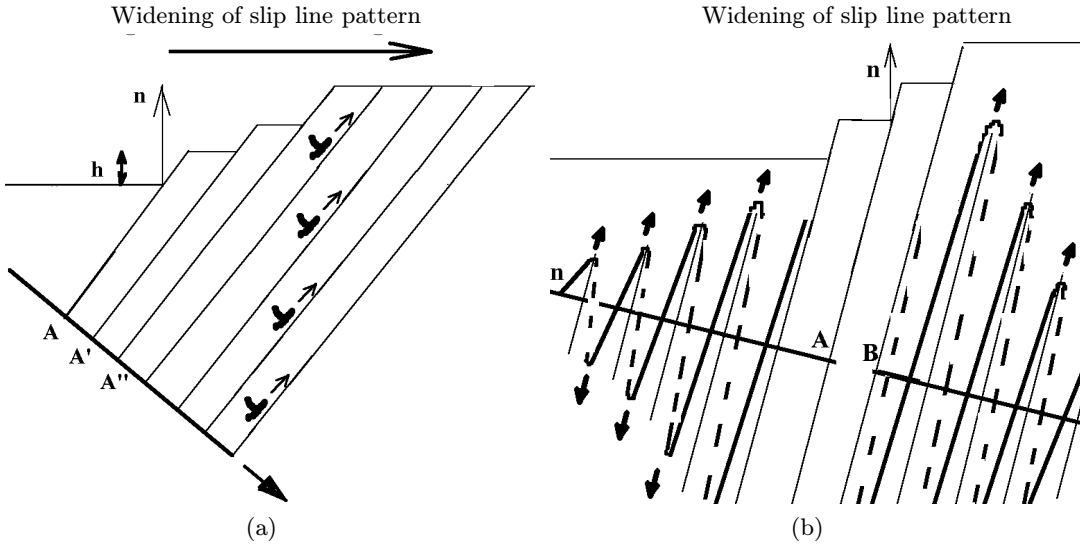

Fig. 7. Step structure generated at the surface resulting from the activation of various dislocation sources for (a) a movable Frank-Read source (b) a helical Frank-Read source.

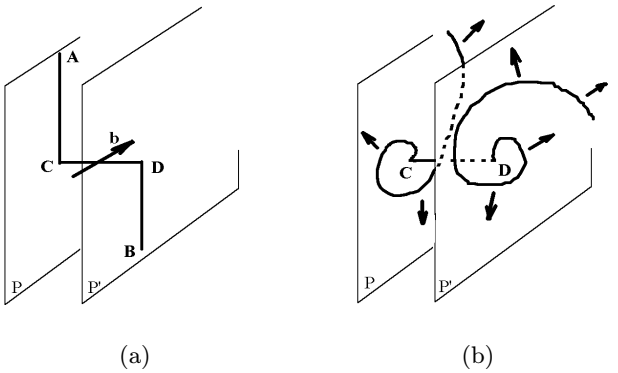

Fig. 8. *Multiple spiral Frank-Read source.* (a) Dislocations AC and BD are glissile, whereas CD is a sessile dislocation segment acting as anchorage for the potential source. (b) Glissile segments expand under stress in a spiral-shape in their own crystallographic slip planes. Each sessile jog along the dislocation line is hence a potential dislocation source, so-called *Multiple spiral Frank-Read source.*

Instead of crossing the dislocation forest, a given gliding dislocation may also pass around this specific cluster, as dislocations around precipitates which leads to Orowan dislocation loops [32]. In the general case of a dislocation cluster $\overline{b}_{\rm s}$ of Burgers vector screw component, where $\overline{b} = \sum_i b_i$ corresponds to the algebraic sum of all dislocation Burgers vector, the initial dislocation will climb on to a parallel crystallographic plane, $\overline{b}_{\rm s}$ apart from the first one considered. This mechanism can be clearly seen by considering the arrangement of atoms around a pure screw dislocation and helical climb of crystallographic planes. Thus the crystal has been sheared twice over and a second step is produced at a distance $\overline{b}_{\rm s}$ from the first one.

It is emphasized that both mechanisms previously described are certainly the main contribution at relatively long range, that is, not on an atomic scale, to the multiplication of slip patterning and widening of step structure at the surface. No effects of Frank-Read source nature are here involved.

All these mechanisms of dislocation multiplication described previously have been implicitly considered to be sources of perfect dislocations. A similar behaviour is obviously suitable to partial dislocations and movable Frank-Read sources can also be thought of as appropriate sources for twinning mechanisms. No cross slip has here to occur, contrary to the Pirouz model which has considered the impossibility after one revolution for a new dislocation to expand once again in the same slip plane, due to the high-staking fault, and therefore the further jump out in a parallel crystallographic plane.

4 Conclusion

The multiplication and widening of slip line structure at the specimen surface is accounted for by both the nature of the Frank-Read sources and the forest interactions of nucleated dislocations before emerging at the free surface. The relative contribution of Frank-Read sources and forest crossing is difficult to estimate, although the interaction with the dislocation network seems to be the main contributor at long range from the initial source, except for sources located near the surface.

Because of its atomic-scale resolution, the atomic force microscope is particularly suited to observe and analyze the fine slip line pattern, but the effects of each factor remain difficult to decorrelate, depending strongly on the studied material. For LiF single crystals, the surface appears homogeneously sheared and the height of the step structure is always very low. No main contribution can thus be emphasized [13]. On the contrary, Ni-based superalloy phase γ is very different with dense step clusters

separated by wide terraces, which suggests a collective behaviour of dislocations by the propagation of planar dislocation pile-ups [9]. Anyway the necessity to complete this analysis with transmission electronic microscopy observations is obvious and may provide considerable information about plastic mechanisms, from the nucleation of the first few dislocations from the bulk crystal, through to the stage of work-hardening and to secondary slip system activation.

The authors would like to thank L. Cartz for fruitful discussions and useful suggestions. This present work was partially supported by the DRET agency and the Région Poitou-Charentes.

References

1. G. Binnig, H. Rohrer, C. Gerber, E. Weibel, Phys. Rev. Lett. **50**, 120 (1983).
2. G. Binnig, C.F. Quate, C. Gerber, Phys. Rev. Lett. **56**, 9 (1986).
3. F.J. Giessibl, G. Binnig, Ultramicroscopy **42-44**, 7 (1992).
4. M. Ohta, T. Konishi, Y. Sugawara, S. Morita, M. Suzuki, Y. Enomoto, Jpn J. Appl. Phys. **32**, 2980 (1993).
5. E. Meyer, H. Heinzelmann, H. Rudin, H.J. Guntherodt, Z. Phys. B **79**, 3 (1990).
6. T. Waitz, H.P. Karnthaler, Acta Met. **45**, 837 (1997).
7. S.Y. Shiryaev, F. Jensen, J.W. Petersen, Appl. Phys. Lett. **64**, 3305 (1994).
8. G. Pezzotti, R. Hiesgen, T. Nishida, Appl. Phys. Lett. **68**, 45 (1993).
9. C. Coupeau, M. Jouiad, S. Brochard, A. Coujou, J. Grilhé, Philos. Mag. A (in press, 1999).
10. L. Ressier, F. Voillot, M. Goiran, J.P. Peyrade, J. Appl. Phys. **79**, 8298 (1996).
11. M.K. Small, C. Coupeau, J. Grilhé, Script. Met. Mat. **32**, 1573 (1995).
12. C. Coupeau, J.C. Girard, J. Grilhé, J. Vac. Sci. Tech. B **16**, 1964 (1998).
13. C. Coupeau, J.C. Girard, J. Grilhé, Probe Microscopy (in the press, 1999).
14. I. Musevic, G. Slak, R. Blinc, Rev. Sci. Instr. **67**, 2554 (1996).
15. W.J. Kulnis, W.N. Unertl, Mat. Res. Soc. Symp. Proc. **332**, 105 (1994).
16. F. Louchet, Solid State Phenom. **35**, 57 (1994).
17. Y. Brechet, G. Canova, L.P. Kubin, Acta Met. Mat. **44**, 4261 (1996).
18. Y. Brechet, L.P. Kubin (private communication)
19. W.T. Read, *Dislocations in crystals* (Mcgraw-Hill, 1953).
20. D. Hull, *Introduction to dislocations* (Pergamon Press, 1975).
21. F.R.N. Nabarro, *The theory of crystal dislocation* (Oxford University Press, 1967).
22. J.P. Hirth, J. Lothe, *Theory of dislocations* (McGraw-Hill, 1968).
23. W.C. Dash, *Dislocations and Mechanical Properties of Crystals* (Wiley, New York, 1957).
24. F. Louchet, J. Phys. C **13**, L847 (1980).
25. P. Pirouz, Script. Met. Mat. **23**, 401 (1989).
26. P. Pirouz, P.M. Hazzledine, Script. Met. Mat. **25**, 1167 (1991).
27. S. Mahajan, G.Y. Chin, Acta Met. Mat. **21**, 1353 (1973).
28. P.B. Hirsh, P.G. Partridge, R.L. Segall, Philos. Mag. A **4**, 721 (1959).
29. G. Saada, Acta. Met. **8**, 841 (1960).
30. J. Friedel, *Internal Stresses, Fatigue in Metals* (North Holland P.C., Amsterdam, 1959).
31. F. Louchet, Solid State Phenom. **35-36**, 57 (1994).
32. E. Orowan, *Fatigue, Fracture of Metals* (Wiley, New-York, 1952).